



Depositional setting of the southern arms of Lago Argentino (southern Patagonia)

Jorge Lozano, Federica Donda, Donald Bran, Emanuele Lodolo, Luca Baradello, Roberto Romeo, Juan Francisco Vilas, Maurizio Grossi & Alejandro Tassone

To cite this article: Jorge Lozano, Federica Donda, Donald Bran, Emanuele Lodolo, Luca Baradello, Roberto Romeo, Juan Francisco Vilas, Maurizio Grossi & Alejandro Tassone (2020) Depositional setting of the southern arms of Lago Argentino (southern Patagonia), Journal of Maps, 16:2, 324-334, DOI: [10.1080/17445647.2020.1746700](https://doi.org/10.1080/17445647.2020.1746700)

To link to this article: <https://doi.org/10.1080/17445647.2020.1746700>



© 2020 The Author(s). Published by Informa UK Limited, trading as Taylor & Francis Group on behalf of Journal of Maps



[View supplementary material](#)



Published online: 28 Mar 2020.



[Submit your article to this journal](#)



[View related articles](#)



[View Crossmark data](#)



Depositional setting of the southern arms of Lago Argentino (southern Patagonia)

Jorge Lozano ^{a,b}, Federica Donda ^c, Donald Bran ^{a,b}, Emanuele Lodolo ^c, Luca Baradello ^c, Roberto Romeo ^c, Juan Francisco Vilas ^{a,b}, Maurizio Grossi ^c and Alejandro Tassone ^{a,b}

^aFacultad de Ciencias Exactas y Naturales, Depto. De Ciencias Geológicas, Universidad de Buenos Aires, Buenos Aires, Argentina; ^bInstituto de Geociencias Básicas, Aplicadas y Ambientales de Buenos Aires (IGeBA), CONICET-Universidad de Buenos Aires, Buenos Aires, Argentina; ^cIstituto Nazionale di Oceanografia e di Geofisica Sperimentale (OGS), Trieste, Italy

ABSTRACT

Lago Argentino hosts a series of calving glaciers originating from the Southern Patagonian Icefield, the largest temperate ice cap of the southern hemisphere. Brazo Rico and Brazo Sur are two basins located in the southern part of Lago Argentino, where a series of high-resolution seismic profiles have allowed reconstruction of its depositional setting and sedimentary architecture, and to produce the following maps: top of the acoustic basement, top of the glacial sequence, and thickness of the glacio-lacustrine deposits. Data reveal the role of basement highs in the complex dynamic behavior of the two main glaciers, Perito Moreno and Frías glaciers, which fluctuated along Brazo Rico and Brazo Sur since the end of the Last Glacial Maximum. Their advances and retreats are testified by the presence of several moraine fronts buried beneath a generally undisturbed, glacio-lacustrine and lacustrine sequence, which records the depositional history of the southern arms of Lago Argentino.

ARTICLE HISTORY

Received 16 December 2019
Revised 19 March 2020
Accepted 20 March 2020

KEYWORDS

Lago Argentino; Brazo Rico; Brazo Sur; high-resolution seismic profiles; contour maps; subaqueous moraines

1. Introduction

Lago Argentino is the second largest lake in Patagonia. It is an almost E–W elongated, structurally-controlled valley, which hosts eight major outlet glaciers of the South Patagonian Icefield (SPI), the largest one being represented by the Upsala glacier, and the most famous being the Perito Moreno glacier. It is generally accepted that the prominent moraine belts that enclose the major Patagonian lakes record the Last Glacial Maximum (LGM), although significant controversy concerning late-glacial dynamics still exists. Well-preserved glacio-genic landforms and stratigraphic exposures provide evidence of repeated glacier advances and retreats after the deep recessional phase into the Andean Cordillera at around 12,650 cal yr PB (Strelin et al., 2011 and references therein). Until now, information on the sedimentary sequences and landforms linked to the dynamics of the glacial fronts were completely missing within the lake. Recently, a geophysical study focused on the analysis of the stratigraphic succession of the south-western branches of the Lago Argentino (Brazo Rico and Brazo Sur) led to the first identification of subaqueous moraine complexes indicative of late-glacial major fluctuations of the Perito Moreno and Frías glaciers (Lodolo et al., in press).

Here we present the main results of the morphological analysis of the whole geophysical dataset collected

by the Istituto Nazionale di Oceanografia e di Geofisica Sperimentale (OGS) and the Instituto de Geociencias Básicas, Aplicadas y Ambientales de Buenos Aires (IGeBA) along Brazo Rico and Brazo Sur. This study has allowed to compile three contour maps of three sequences (Main Map), which record key features related to the glacial history of the study area: (1) the isochron map of the acoustic basement; (2) the isochron map of the top of the ancient glacial deposits; and (3) the isopach map of the glacio-lacustrine deposits. Although we do not have precise calibrations to associate an age to the various sedimentary bodies related to the Perito Moreno and former Frías glaciers fluctuations within the general phase of late Pleistocene–Holocene regression, these maps allow us to reconstruct, at least in part, their complex post-LGM dynamics, and to highlight the different depositional environments in this sector of southern Patagonia.

2. Physiographic and geological setting

Lago Argentino is a large ice-contact proglacial lake into which eight outlet glaciers flow from the SPI. The eastern part of the lake is characterized by a large single basin within a semi-arid steppe climate, whereas to the west the lake is segmented into several arms that extend into the Andes foothills under wetter

conditions. Brazo Rico and Brazo Sur comprise E-W and N-S trending longitudinal basins, respectively, and are located in the southern part of Lago Argentino (Figure 1).

The glacial troughs of Brazo Rico and Brazo Sur are carved into turbiditic rocks of the Cerro Toro Formation, which has an Upper Cretaceous age (Nullo et al., 2006). These rocks formed in a N-S trending compressional phase that created a system of fold and thrust belt developed during distinct stages of the Andean orogeny that occurred until the Pliocene (Ghiglione et al., 2016; Giacosa et al., 2012). During the Quaternary, the glaciers expanded their fronts towards the east (Rabassa et al., 2011; Strelin et al., 2014, 2011) and both arms of Lago Argentino, along with the other narrow valleys, were entirely covered by ice. The last glaciation, known in the area as El Tranquilo Glaciation (Strelin & Malagnino, 1996), reached its maximum extent at nearly 15 ^{14}C kyr BP (Glasser et al., 2004). Whenever possible, the radiocarbon ages discussed in the text are given as calibrated ages, cal BP. Otherwise, we will refer to the original conventional ^{14}C BP. After the LGM, the ice-lobes experienced a major recession stage, interrupted at nearly 11 ^{14}C kyr BP when a glacier re-advance stage occurred (Strelin et al., 2011). This stage is recognized to the east of Brazo Rico, where the Puerto Bandera 1 moraine has been identified and mapped. Afterwards, recession from this point was characterized by oscillations of the ice-front that resulted in the formation of Puerto Bandera 2 and 3 moraines (Mercer, 1968; Strelin et al., 2011). During the Holocene, the Lago Argentino outlet glaciers underwent repeated episodes of advance and retreat after the marked recessional phase into the Andean Cordillera at around 12,650 cal yr BP (Strelin et al., 2011).

Nowadays, the Perito Moreno Glacier front lies in the westernmost part of the Brazo Rico and in the southernmost part of Canal de los Témpanos (Figure 1). This glacier is widely known by its minor fluctuations of the calving ice-front that produces ice-damming phenomena, isolating the Brazo Rico and Brazo Sur from the rest of Lago Argentino (Skvarca & Naruse, 1997). Semi-periodical ruptures of the glacier front have occurred a number of times over at least the last 80 years, producing spectacular water outbursts from the two arms of the lake into the Canal de los Témpanos (Guerrido et al., 2014).

3. Materials and methods

3.1. Equipment

All seismic profiles (Figure 1) were acquired in the southern arms of Lago Argentino with an EPC boomer system with a transducer of 0–2.5 kV. It consists of an electromagnetically-driven sound plate mounted on a towed catamaran and a separate streamer (hydrophones

array) for receiver. The acoustic pulse is generated when a capacitor bank discharges through a flat spiral coils which quickly moves an aluminum plate. The pulse is very short (normally with length of 100–200 μs) in a frequency range of 400–4000 Hz, and has a clean signature and good repeatability. This large frequency band can produce a decimetric vertical resolution. In our surveys, we used a multi-channel MicroEel Streamer by Geometrics as a receiver. This solid-state streamer has 8 channels with inter-trace of 3.15 m and each channel is composed by 4 hydrophones (–196 dB re 1 V/1 μPa sensitivity). The acquisition system was a Geode Geometrics with 24 bits A/D convert. The Seismodule Controller Software (SCS) Geometrics in a Windows environment PC collected and stored the acquired seismic data in SEG-Y – IBM format. This software allows one to perform quality-control in real time of single shot and shows the near trace in a continuous mode. A DGPS AgGPS123-Trimble interfaced with the SCS has guaranteed the positioning of the collected tracks. To plan and follow the routes we used the NavPro (Communication Technology) on a laptop. The acquisition geometry adopted during the survey was a classic streamer behind the plate with a near offset of 12 m and a lateral offset of 2 m. Data were acquired with a sampling rate 0.125 ms, shooting every 1.5 s and a record length of 700–800 ms. The boat used for the surveys (Zodiac) kept an average ship speed between three and four knots (inter-trace range from 2.2 to 3 m).

3.2. Data processing

All datasets were processed with Echos (Paradigm) on a workstation Linux with a standard sequence. The first step was to convert all geographic WGS84 coordinates to UTM 19 WGS84 and associate them to each trace. After gain (spherical divergence and inversion curve) and filtering (DC-removal and band-pass) were applied, to eliminate electrical noise an algorithm that create gathers common offset and transform to time–frequency domain within short windows by using FFT was used. In every window, the median of the amplitude spectrum is calculated in several frequency sub-bands. The noise threshold (NT) is defined as the median of all medians. In each sub-bands, the algorithm accepts any spectral amplitude value less than NT and scales any spectral amplitude value exceeding NT. The inverse FFT yields the filtered data in TX domain. To increase vertical resolution, a deconvolution filter based on Wiener-Levinson was designed and used. We tested several predictive deconvolution parameters, and finally we adopted a 9 ms operator length, 0.6 ms gap length with 0.1 percentage of white noise. Several predictive deconvolution parameters were tested. Finally, 9 ms operator length, 0.6 ms gap length with 0.1 percentage of white noise were adopted.

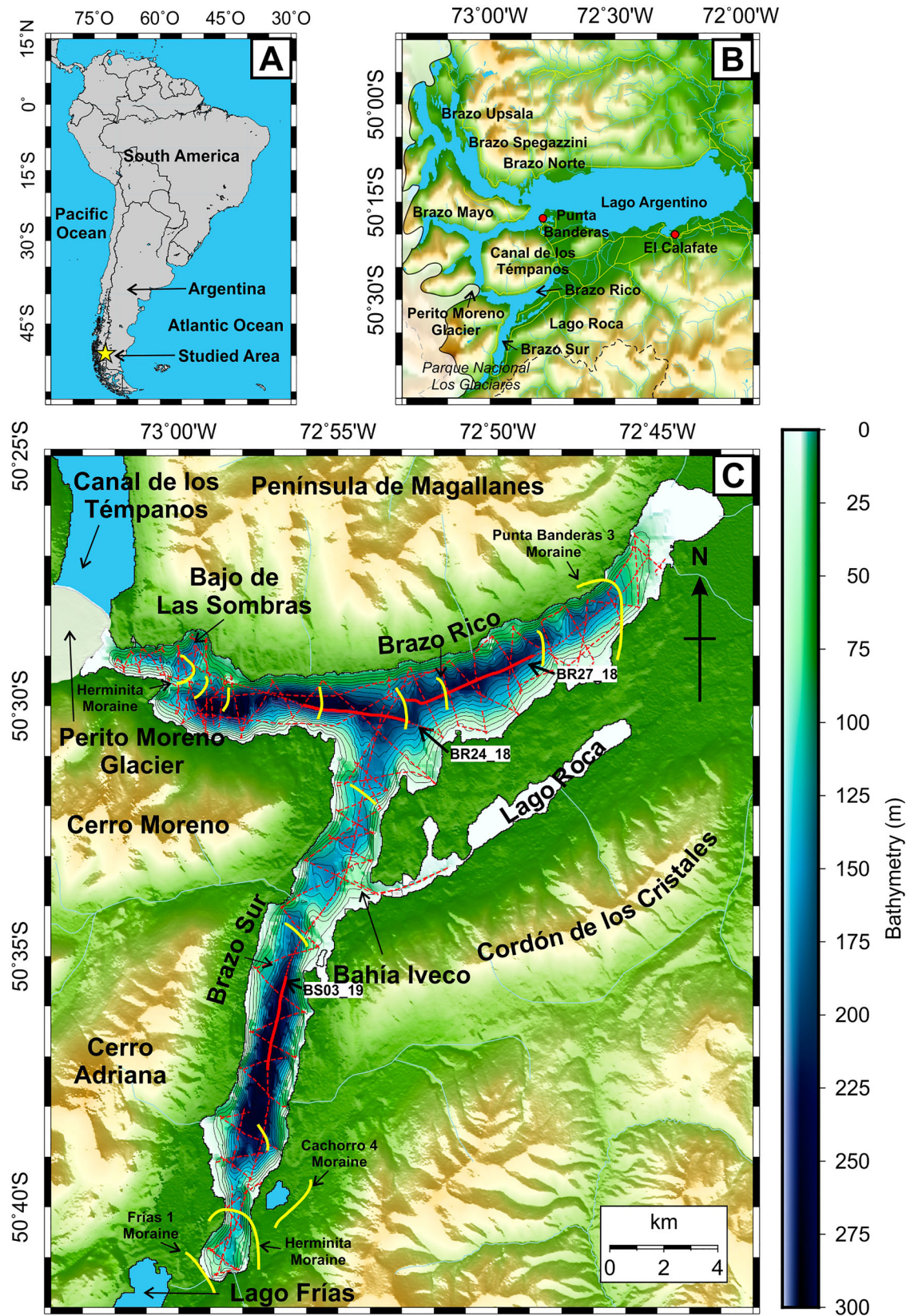


Figure 1. (A) Location of the studied area in the southernmost South America. (B) Lago Argentino, in Provincia de Santa Cruz, Argentina. (C) Main geographic references in the surroundings of Brazo Rico and Brazo Sur, the studied lake arms. The yellow lines shows the location of the moraines system identified in the seismic lines; red lines shows the location of the seismic sections; thicker red continuous lines show the position of the seismic profiles displayed in Figure 4.

3.3. Velocity analysis

The acquired data were sorted by Common Depth Point (CDP) and a velocity analysis was performed

with a Constant Velocity Analysis (CVA) and not only with traditional Semblance (Yilmaz, 2001). We used this approach because the CDP fold is low and

data do not have long offsets with respect to lake depth to have good semblances. We considered a group of adjacent CDP (Super Gather) around the location point where we wanted to know the seismic velocity. In a range of acoustic velocity (1400–1800 m/s) the CVS algorithm corrects Normal Move Out data with scans of 200 m/s and stacks creating several panels. Analyzing stack panels, we chose and pick the velocities where reflections events show the highest amplitude and continuity (Figure 2). Subsequently, the best stack velocity found can be converted into an interval velocity (Dix, 1955) and used to calculate the thicknesses of the various sediments layers. We calculated velocity profiles in several areas along Brazo Rico and Brazo Sur where the sedimentary thickness was greater. The interval velocity values range from 1500 m/s in the sub-superficial part to 1900 m/s in the deepest part (see table in Figure 2). To convert to thickness of the sedimentary cover we used the mean velocity of 1650 m/s, calculated from the weighted average. After apply the dynamic correction for normal move out, we performed the stack sections using a median stack algorithm (it uses the median rather than the average to construct each output sample).

To increase the information for the interpretation, the time sections were migrated with a phase-shift algorithm (Gazdag, 1978). We preferred this tool because its represents an accurate method to migrate

zero-offset seismic data. It works in the frequency domain and solves very accurately the specific conditions with laterally invariant velocities. Figure 3 shows an example of phase-shift migration, where the diffraction hyperbolas are collapsed showing the reflectors continuities.

3.4. Seismic characteristics of the mapped sequences

The analysis of the whole geophysical dataset collected in the study area allowed us to identify three main depositional sequences, bounded by regional-scale seismic horizons. They record a marked change in the seismic-stratigraphic characteristics of the surveyed area, which reflect changes in the lithology, geometry and distribution of the deposits, as a consequence of variations in environmental conditions within the basin. The seismic horizons bounding these sequences are the top of the acoustic basement (U1, later called ‘Basement’) and the top of the old glacial units (U2, later called ‘Glacial Unit’).

The top of the acoustic basement (U1) consists of a high amplitude reflection, with a very irregular surface. The difference in depth between highs and lows reaches almost 450 ms in places (Figure 4(A,B)). It is important to clarify that the acoustic basement does not necessarily coincide with the lithologic basement

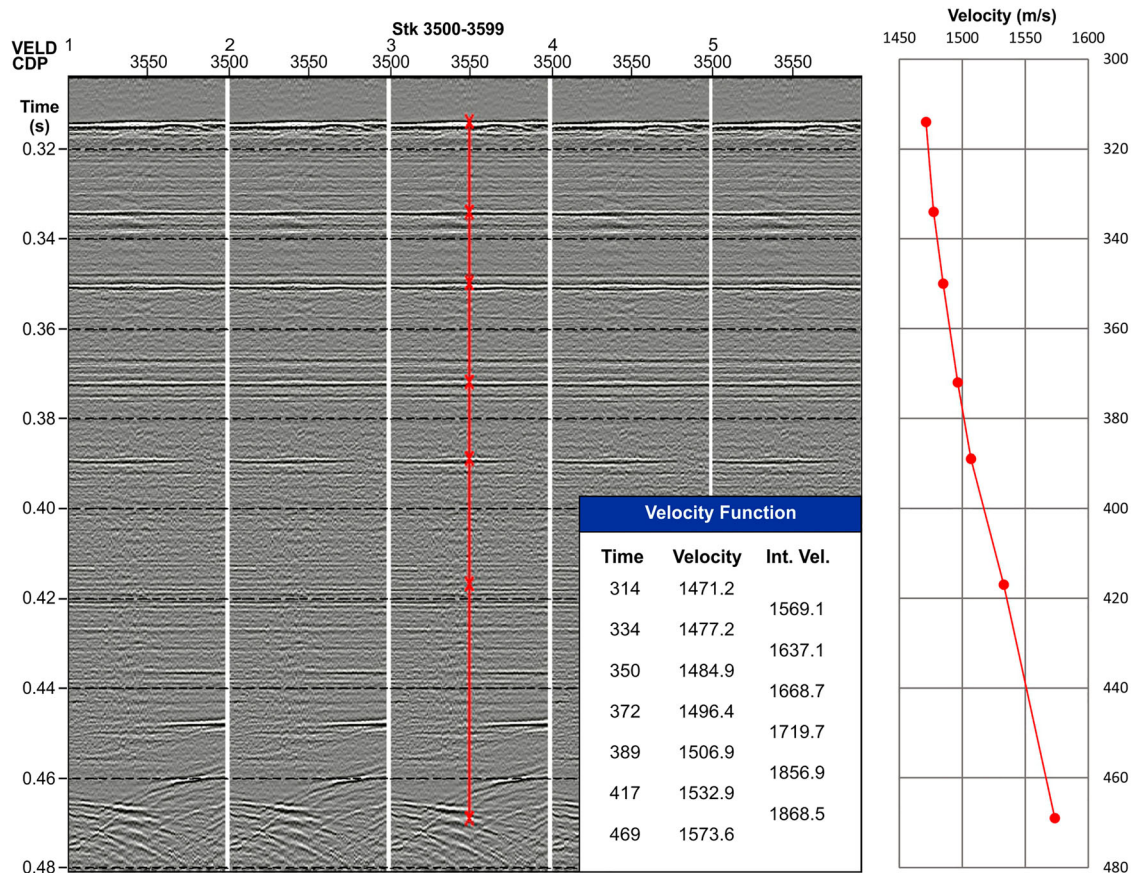


Figure 2. An example of CVS analysis on BR_27_18 profile on sediments basin. The five panels show different stacks when the velocity range change. The central panel is the best stack section with the velocity field shown in table (stack and interval velocities).

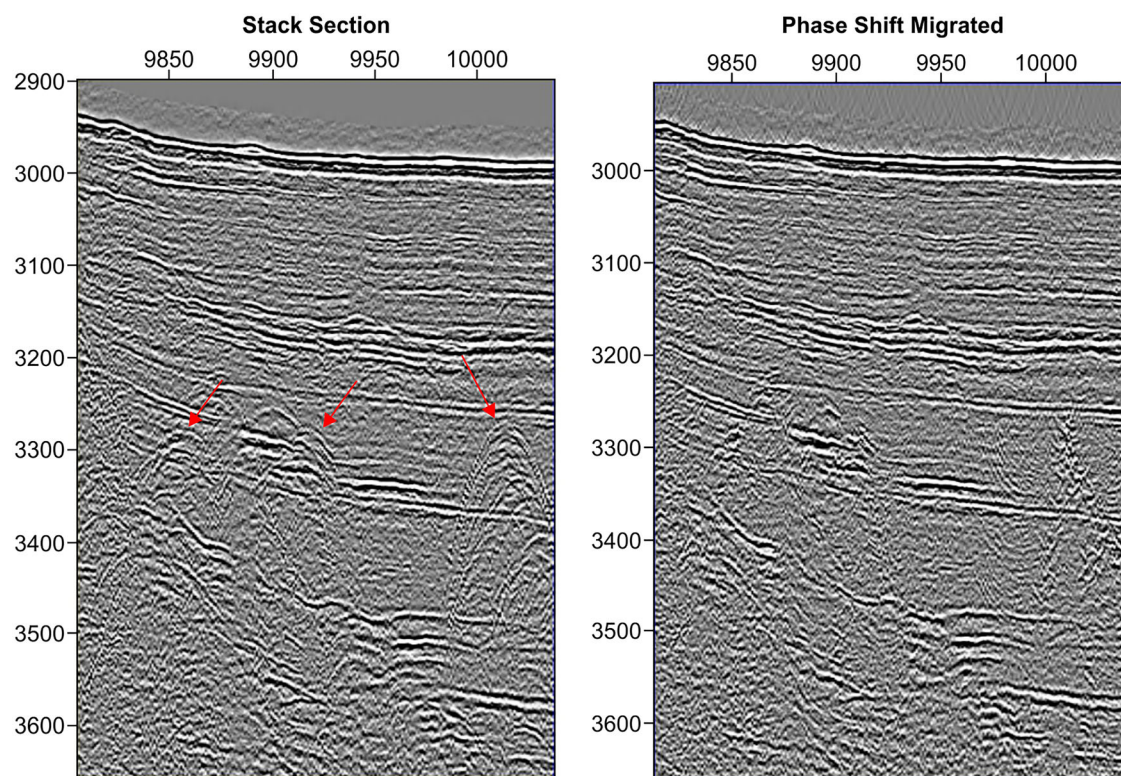


Figure 3. A detail of seismic profile BR24_18: Stack section (left) and phase shift migrated. All diffraction hyperbolas are collapsed and the reflectors have better resolution. The red arrows highlights the location of the diffraction hyperbolas.

in the area, which is composed by mudstones and sandstones from the turbiditic deposits of the Upper Cretaceous Cerro Toro Fm., cropping out in the Magallanes Península and Cerro Moreno (Nullo et al., 2006). Often, this reflector is not recognizable, since it amalgamates with the overlying chaotic facies (Figure 4(A)) U1 is the lowest, coherent acoustic signal identifiable on the seismic data; underneath it, rare, discontinuous low-amplitude reflections with a chaotic configuration are recognizable in places, since, commonly, this surface marks the top of a reflection-free facies (Figure 4(A,B)). Diffractions are common, especially in correspondence to the ridges (Figure 4(C)). The U1 reflector has been identified both within the central part of the lake arms and along the lakeshores. Basement highs commonly outcrop in the Brazo Rico, with highs up to 75 m, and separate several sub basins. Locally, these highs can be correlated to promontories that extend from onshore into the lake body. Often, basement highs are overlain by mound-shaped features, within both the upper seismic sequences and the lake floor (Figure 4(A,B)). This reflector is interpreted as the top of the Mesozoic deformed units, overlain by ice-contact/glacial deposits. The basement characteristics appear to be very similar in its acoustic facies to those observed in Lago Fagnano (Waldmann et al., 2010).

The horizon U2 is represented by a highly irregular, high amplitude seismic reflector, on top of a

commonly chaotic facies, constituted by irregular, medium to high amplitude reflectors, revealing mound-shaped features (Figure 4(D)). Along the length of both of the studied lake arms, U2 reliefs often are present just above the basement highs (Figures 4(A,B)). This horizon also constitutes the base of the overlying well-stratified facies described below as glacio-lacustrine deposits, but, locally, it almost crops out (Figures 4(A,B)).

The overall complex morphological and acoustic characteristics of the seismic sequence bounded by U2, i.e. the Glacial Unit, suggest that it represents glacial deposits, with the mound-shaped reliefs being moraines, similar to how crested morphologies identified in the Lago Fagnano has been interpreted (Waldmann et al., 2010), as well as in alpine lakes (Fabbri et al., 2018) and other perialpine lakes (Dowdeswell et al., 2016; Hilbe et al., 2016). However, we cannot differentiate seismically whether they represent frontal or recessional moraines. These appear to be larger and more widespread with respect to the ones located on the lake floor (i.e. Lodolo et al., in press) but, similar to these, these are well preserved. Due to these characteristics, we suggest that these glacial deposits bounded by the U2 reflector record the past fluctuations of both the Frías and Perito Moreno glaciers possibly within the general post-LGM retreat phase.

Above the Glacial Unit, medium to high amplitude, continuous, sub-horizontal reflectors are well imaged on the seismic profiles in the whole study area. They

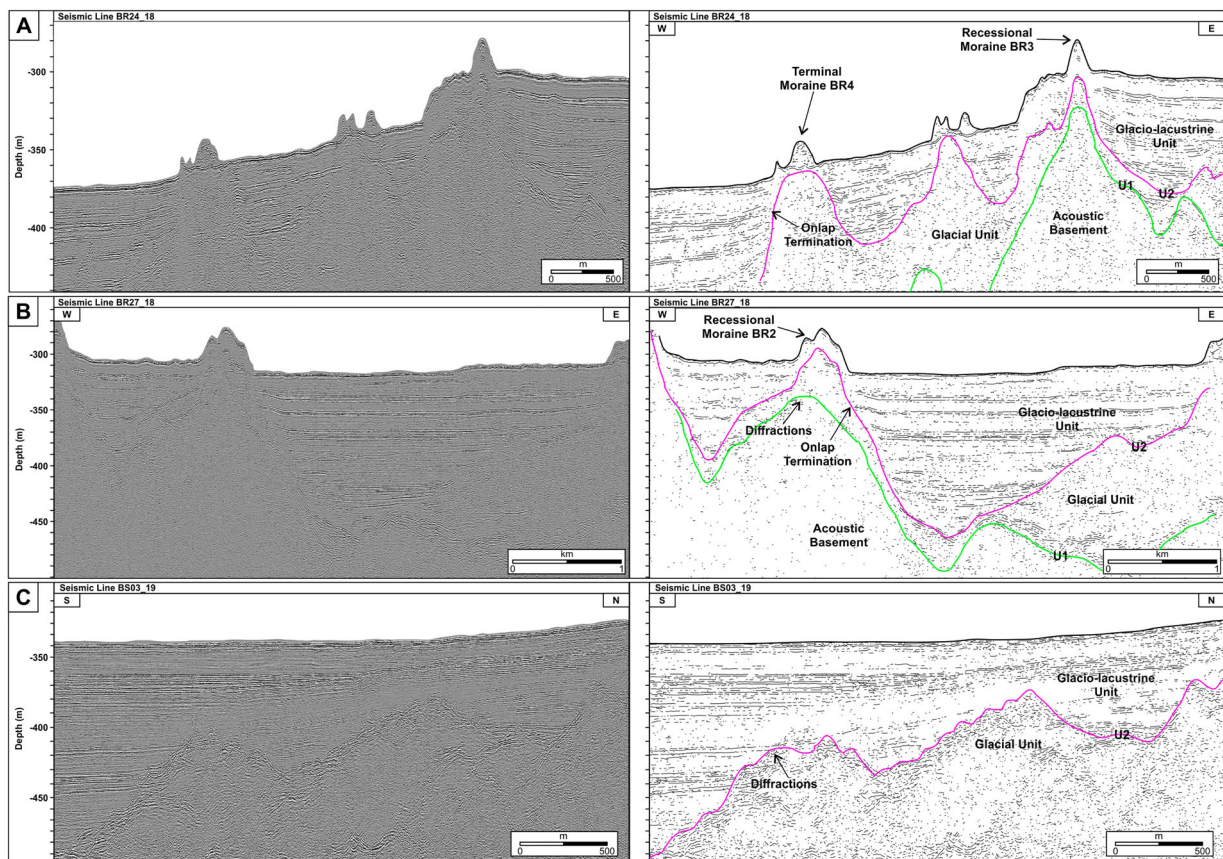


Figure 4. Examples of seismic sections along Brazo Rico and Brazo Sur. The right side of the insets shows the line drawing of the interpreted seismic section. (A) BR24_18. Part of the seismic line collected at the confluence between the Brazo Rico and the Brazo Sur, where both the U1 and U2 reflectors have been identified. The image clearly shows the role of the basement high in the formation of an ancient moraine body and that deposited on the lake floor (i.e. SP7750). Other moraine systems are identifiable at the lake floor, where the top of the Glacial unit is almost outcropping. (B) BR27_18. Part of the seismic line collected along the eastern arm of the Brazo Rico, where both the U1 and U2 reflectors have been identified. The image clearly shows that both the ancient moraine bodies and those deposited on the lake floor formed just above the basement high. Glacio-lacustrine deposits reach here a thickness of about 110 m. On the left, the low-relief, convex-upward chaotic facies at the lake floor would represent a slide of sediments possibly originating from the lakeshore. (C) BS03_19. Part of the seismic line collected along the Brazo Sur, where the U2 reflector has been identified. Glacial deposits below of it are characterized by an overall irregular morphology, where mounded-shaped features can be recognized. Glacio-lacustrine deposits above of the 'Glacial' are constituted by both sub-parallel and slightly inclined horizons, and an erosional unconformity, at ca. 0.37 ms, which would possibly indicate a lower lake stand. The moraines were named following the nomenclature for the moraine ridges from [Lodolo et al. \(2020\)](#).

fill the morphological lows, as revealed by onlap reflector configurations (Figure 4(D,B)). According to [Waldmann et al. \(2010\)](#) we interpret this facies as representing glacio-lacustrine deposits, which record the sedimentary emplacement of the Lago Argentino in these southern arms. Sediment thickness within confined basins reaches up to 120 m (with a mean seismic velocity of 1650 m/s) (Figure 4(D,B)).

Within the glacio-lacustrine deposits, several higher amplitude reflectors are identifiable (Figure 4 (A,B,D)). Among them, a basin-wide seismic horizon has an evident erosional character, since it locally truncates underlying reflectors, whereas above it onlap reflector configurations have been identified (Figure 4(B)). This unconformity can be traced along both the lake arms, and is commonly found at a depth of 12-13 ms two-way traveltime (TWT) below the lake floor. However, in the central part of Brazo Sur, the discontinuity deepens, reaching

22 ms TWT below the lake floor. The characteristics of this unconformity suggest that it records a lower water lake stand at this time.

3.5. Map production procedure

The entire seismic survey was uploaded into a IHS Markit Kingdom software project, where the seismic lines were visualized and the U1 and U2 horizons were then picked. These geo-referenced horizons were exported with their time-attributes and merged with the vector shape of Brazo Sur and Brazo Rico from the SWBD (SRTM Water Body Data, NASA 2003) to have well-constrained points for the development of grids. The data between the measured points and the lake margins were interpolated using the Kriging method with search parameters using an ellipse radius elongated according to the direction of the Brazo Rico (E-W) and Brazo Sur (N-S).

The result of this procedure was the compilation of two-way traveltime (TWT) grids with 0.001° spacing for: (i) the top of the acoustic basement, (ii) the top of the glacier unit: and (iii) the thickness of the glacio-lacustrine sequence. An analogous methodology was applied in the lakes of Tierra del Fuego, like Lago Fagnano (Esteban et al., 2014), Lago Yehuín (Lozano et al., 2018a), Lago Chepelmut (Lozano et al., 2018b) and Lago Roca (Bran et al., 2019).

The thickness maps were calculated as the difference between two adjacent TWT grids. The resulting grids were filtered to delete artifacts generated from the grid operations. Specifically, the glacio-lacustrine thickness (in TWT) grid was converted to meters using the interval acoustic velocity described above.

4. Contour maps

4.1. Top basement map

Figure 5 shows the map of the top of the acoustic basement with depths expressed in TWT (s). The white-masked areas are the sectors where the seismic data does not allow to recognize the U1 reflector. The map is strictly developed using measured points along the southern arms with the aim of avoiding extrapolation of the data.

The acoustic basement is characterized by a maximum depth of almost 650 ms TWT near the southern side of Brazo Sur. In Brazo Rico, the maximum depth is less, approximately 55 ms TWT next to the intersection between both the southern arms.

The morphology of the acoustic basement is in concordance with the shape of the lakes, forming trench-like depressions elongated in the central axis of the arms. These depressions are irregular and are compartmented into a few sub-basins, separated by basement highs. The recognized main highs are located in Brazo Sur, next to the entrance to Lago Roca and in the crossing between the southern arms, where two sub-basins can be recognized eastwards and westwards along Brazo Rico (Figure 5).

4.2. Top Glacial map

The map of the glacial top (U2) is shown in Figure 6. The distribution of this reflector corresponds well with the acoustic basement map (Figure 5). The maxima depth values of the Glacial horizon are between 450 and 500 ms TWT in the southern side of Brazo Sur and in the eastern and western part of Brazo Rico. The morphology of U2 shows the presence of a few ridges separated by the basement highs recognized

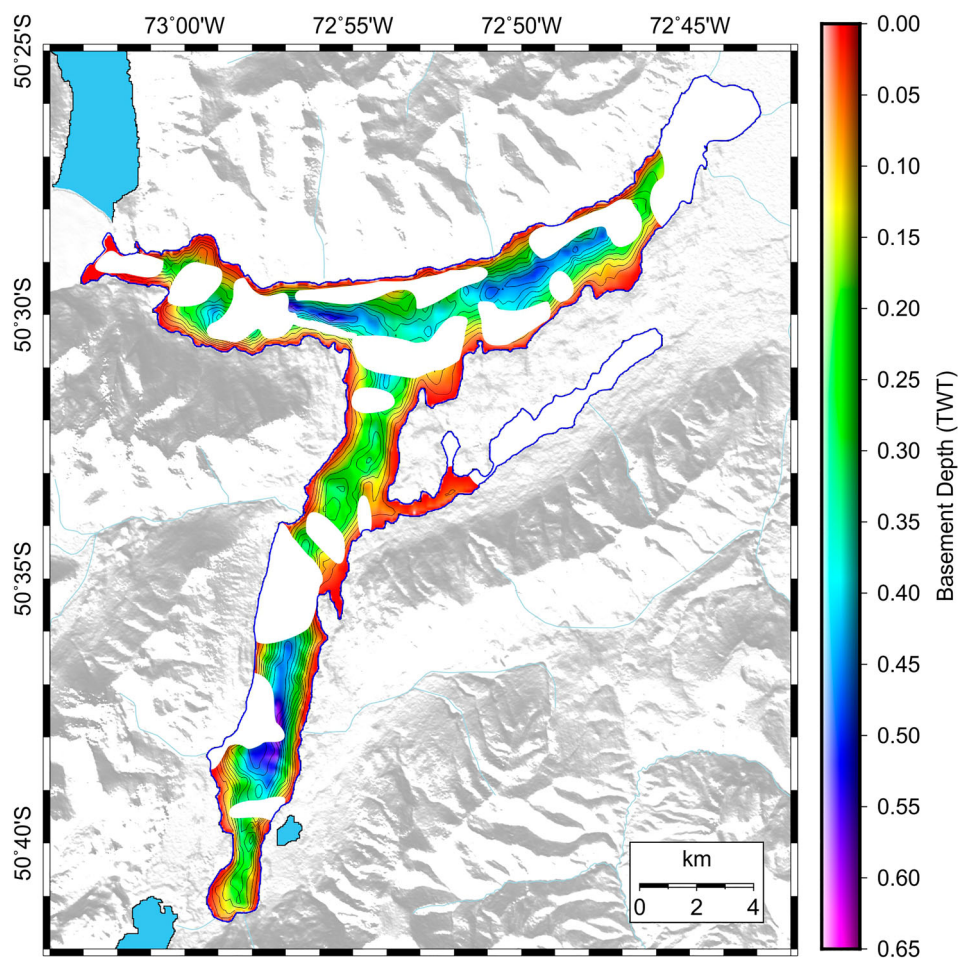


Figure 5. Top basement map of the southern arms of Lago Argentino, expressed in TWT (s). The white areas shows the position in which the acoustic basement cannot be recognized.

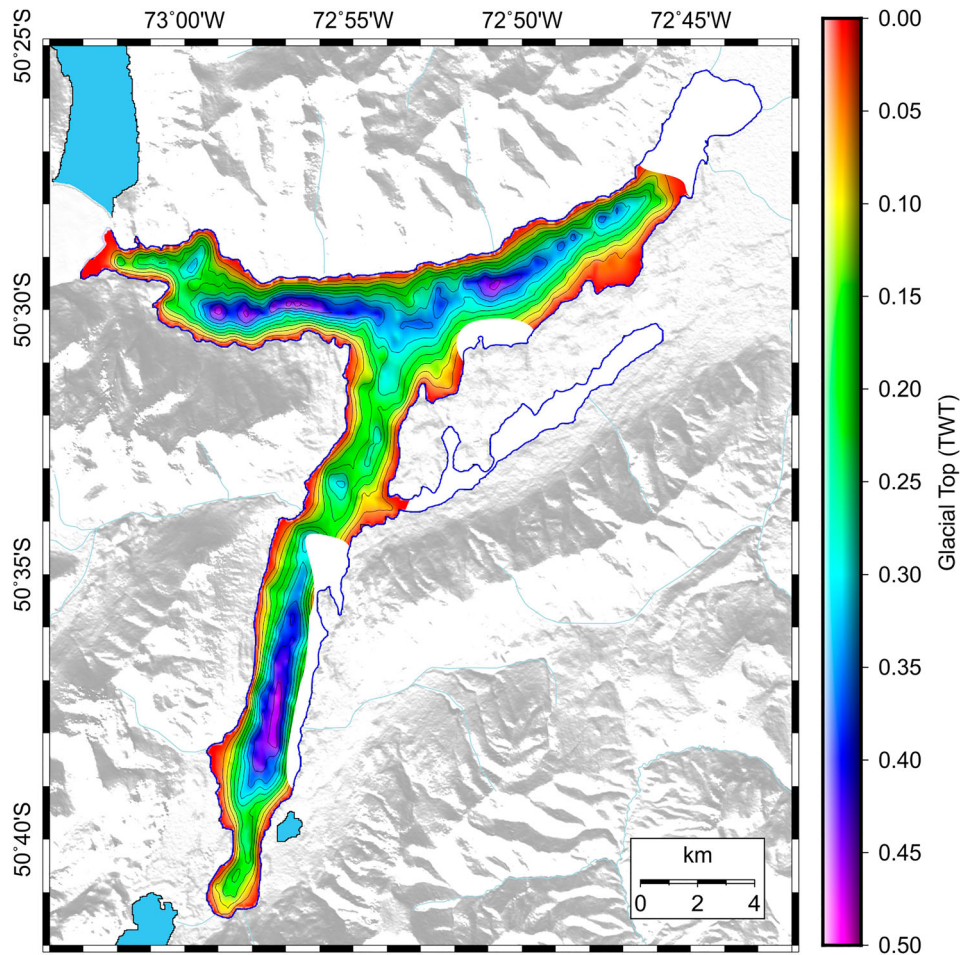


Figure 6. Map of the top of the glacial unit (U2) along Brazo Rico and Brazo Sur, expressed in TWT (s). The white areas shows the position in which the horizon cannot be recognized.

in Figure 5. Next to the intersection between Brazo Rico and Brazo Sur, U2 is shallower, at lies approximately at 350 ms TWT. Southwards of this area and close to Bahía Iveco (non-formal toponym), U2 progressively shallows to depths between 100 and 250 ms TWT.

There is a correlation between the basement morphology and the distribution of the glacial top, i.e. morphological highs of Glacial Unit occur for the most cases above the basement highs. We suggest that the highs in the basement morphology may have controlled the dynamic behavior of Perito Moreno and Frías glaciers since the end of the Last Glacial Maximum, thus acting as pinning points (Benn et al., 2017; Favier et al., 2014), which in turn led to deposition of the moraine systems within the glacial unit along both the Brazo Rico and Brazo Sur.

4.3. Isopach map of glacio-lacustrine deposits

The high resolution seismic data were used to recognize the Lago Argentino infill represented by glacio-lacustrine deposits. The related isopach map (Figure 7) shows the distribution of these deposits, characterized by horizontal to sub-horizontal, continuous and almost

undeformed reflectors, locally infilling confined basins, which are widespread along Brazo Rico and Sur.

The shape of the basins is commonly sub-circular, especially for the small ones, while in the larger ones, the shape appears to be elongated along the central axis of the lake arms. In the Brazo Rico, the largest basin is *ca.* 3.3 km in length, while in the Brazo Sur, the largest basin is almost 8 km in length. The distribution of the isolated basins along Brazo Sur is quite irregular, but they are mostly found in the center of the lake. Eastwards of Brazo Rico, the basins are located next to the northern slope.

The thicker deposits in the Brazo Sur (>100 m) are located southwards, in agreement with the deeper position of both U2 and U1, and additionally, in the central axis of the lake arm. Near Bahía Iveco (Figure 1), there are some isolated small basins with deposits thicker than 50 m. Along Brazo Rico, the thicker glacio-lacustrine deposits can be found in the central-eastern part of the lake arm, reaching almost 125 m in thickness.

We suggest that the glacio-lacustrine deposits represent slow sedimentation of fine to very fine particles due to decantation (Renaut & Gierlowski-Kordesch, 2010). These deposits show a drastic change from the

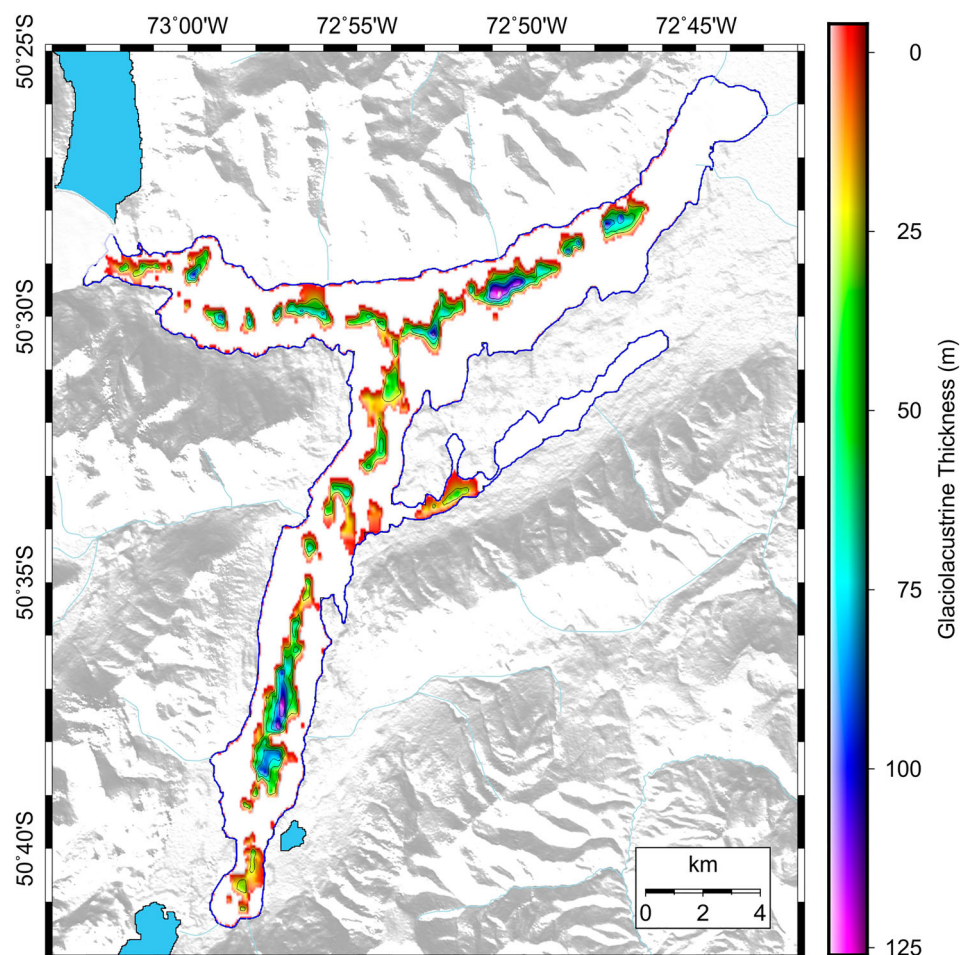


Figure 7. Thickness of the glacio-lacustrine deposits along Brazo Rico and Brazo Sur.

sedimentation associated with the glacial dynamics to a younger lacustrine setting.

5. Conclusions

The high-resolution seismic data acquired in the Brazo Rico and Brazo Sur allowed us to produce three contour maps, which in turn allowed us to reconstruct the overall morphology and depositional setting of the southern part of Lago Argentino for the first time. The map of the top of the acoustic basement clearly reveals the key role of basement highs in the architecture of overlying glacial deposits, in which moraine systems commonly formed just above the basement highs. This suggests that basement highs acted as pinning points, controlled glacier dynamics and, possibly, the glaciers extent during their fluctuations, especially along the Brazo Rico, where basement highs are more prominent.

The isopach map of the glacio-lacustrine deposits allows the identification of confined basins along both Brazo Rico and Brazo Sur, which would hold an expanded and well preserved sedimentary succession. It potentially contain a good paleoclimate and paleoceanographic record, characterized by depositional process that appear to be continuously acting over

the same site for a long time span, thus representing key locations for future sample locations. These maps may thus provide a key reference point for further studies focused on reconstructing the glaciers dynamics along the southern arms of Lago Argentino, which could significantly contribute to improving the knowledge of the Patagonian late-glacial history.

6. "Software"

The high resolution seismic profiles were acquired with the Seismodule Controller Software (Geometrics). The seismic data were processed with Echoes (Paradigm) and interpreted using Kingdom Seismic Package and Geological Interpretation Software IHS Markit. The Golden Software Surfer was used to generate all the interpolated data grids. Finally, the GMT software (Wessel & Smith, 1991) was used to generate all the maps presented in this work.

Acknowledgements

This study is part of a joint Italian-Argentinean 'Grande Rilevanza' scientific project financed by the *Italian Ministero degli Affari Esteri e della Cooperazione Internazionale* (MAECI) and the *Ministerio de Ciencia, Tecnología e Innovación Productiva* (MINCYT) of Argentina, and the project

from *Universidad de Buenos Aires* (UBA), UBACyT N° 20020170100720BA ‘*Estudio geofísico y geológico de Lagos Patagónicos*’. We want to thank the *Prefectura Naval Argentina* for the support provided for the acquisition of the seismic data, and the *Administración de Parques Nacionales* for the permissions provided for the field work in *Parque Nacional Los Glaciares*. Also, we want to thank Dr Paul Dunlop, Dr Anna Labetski, Dr Sara Benetti and the Associate Editor, Dr Jasper Knight, for their observations and corrections that were very helpful to improve significantly this work. In addition, we want to thank the editor in chief, Dr Mike J. Smith, for his support with the editorial process. Finally, we also thank IHS Markit for providing an academic license for Kingdom-Seismic & Geological Interpretation Software.

Disclosure statement

No potential conflict of interest was reported by the authors.

Funding

This study is part of a joint Italian-Argentinean “Grande Rilevanza” scientific project financed by the Italian Ministero degli Affari Esteri e della Cooperazione Internazionale (MAECI) and the Ministerio de Ciencia, Tecnología e Innovación Productiva (MINCYT) de Argentina [Grande Rilevanza 2017-2019, Storia dei ripetuti collapsi della barriera di ghiaccio del Perito Moreno nel Lago Argentino], and the project from *Universidad de Buenos Aires* (UBA) [UBA-CyT N° 20020170100720BA, *Estudio geofísico y geológico de Lagos Patagónicos*].

ORCID

Jorge Lozano  <http://orcid.org/0000-0002-2626-4253>
 Federica Donda  <http://orcid.org/0000-0002-1284-5866>
 Donald Bran  <http://orcid.org/0000-0002-7093-2183>
 Emanuele Lodolo  <http://orcid.org/0000-0002-4706-2095>
 Luca Baradello  <http://orcid.org/0000-0002-9796-4521>
 Roberto Romeo  <http://orcid.org/0000-0001-5867-8998>

References

- Benn, D. I., Cowton, T., Todd, J., & Luckman, A. (2017). Glacier calving in Greenland. *Current Climate Change Reports*, 3(4), 282–290. <https://doi.org/10.1007/s40641-017-0070-1>
- Bran, D. M., Lozano, J. G., Civile, D., Lodolo, E., Cerrredo, M., Tassone, A., Baradello, L., Grossi, M., & Vilas, J. F. (2019). Post-LGM evolution of a ‘fjord-type’ lake based on high-resolution seismic data: The Lago Roca/Acigami (southern Tierra del Fuego, Argentina/Chile). *Journal of Quaternary Science*. <https://doi.org/10.1002/jqs.3179>
- Dix, C. H. (1955). Seismic velocities from surface measurements. *Geophysics*, 20(1), 68–86. <https://doi.org/10.1190/1.1438126>
- Dowdeswell, J. A., Canals, M., Jakobsson, M., Todd, B. J., Dowdeswell, E. K., & Hogan, K. A. (2016). Atlas of submarine Glacial landforms: Modern, quaternary and ancient. Geological Society, London. *Memoirs*, 46, <https://doi.org/10.1144/M46>
- Esteban, F. D., Tassone, A., Lodolo, E., Menichetti, M., Lippai, H., Waldmann, N., Darbo, A., Baradello, L., & Vilas, J. F. (2014). Basement geometry and sediment thickness of Lago Fagnano (Tierra del Fuego). *Andean Geology*, 41(2), 293–313. <https://doi.org/10.5027/andgeoV41n2-a02>
- Fabbri, S. C., Buechi, M. W., Horstmeyer, H., Hilbe, M., Hübscher, C., Schmelzbach, C., Weiss, B., & Anselmetti, F. S. (2018). A subaquatic moraine complex in overdeepened lake Thun (Switzerland) unravelling the deglaciation history of the Aare Glacier. *Quaternary Science Reviews*, 187, 62–79. <https://doi.org/10.1016/j.quascirev.2018.03.010>
- Favier, L., Durand, G., Cornford, S. L., Gudmundsson, G. H., Gagliardini, O., Gillet-Chaulet, F., Zwinger, T., Payne, A. J., & Le Brocq, A. M. (2014). Retreat of Pine Island Glacier controlled by marine ice-sheet instability. *Nature Climate Change*, 4(2), 117–121. <https://doi.org/10.1038/nclimate2094>
- Gazdag, J. (1978). Wave equation migration by phase shift. *Geophysics*, 43(7), 1342–1351. <https://doi.org/10.1190/1.1440899>
- Ghiglione, M. C., Ramos, V. A., Cuitiño, J., & Barberón, V. (2016). Growth of the southern Patagonian Andes (46–53°S) and their relation to subduction processes. In A. Folguera, M. Naipauer, L. Sagripanti, C. Ghiglione M, D. Orts, & L. Giambiagi (Eds.), *Growth of the Southern Andes*. Springer Earth System Sciences (pp. 201–240). Springer.
- Giacosa, R., Fracchia, D., & Heredia, N. (2012). Structure of the southern Patagonian Andes at 49°S, Argentina. *Geologica Acta*, 10, 265–282. <https://doi.org/10.1344/105.000001749>
- Glasser, N. F., Harrison, S., Winchester, V., & Aniya, M. (2004). Late Pleistocene and Holocene palaeoclimate and glacier fluctuations in Patagonia. *Global and Planetary Change*, 43(1–2), 79–101. <https://doi.org/10.1016/j.gloplacha.2004.03.002>
- Guerrido, C. M., Villalba, R., & Rojas, F. (2014). Documentary and tree-ring evidence for a long-term interval without ice impoundments from Glaciar Perito Moreno, Patagonia, Argentina. *The Holocene*, 24(12), 1686–1693. <https://doi.org/10.1177/0959683614551215>
- Hilbe, M., Strupler, M., Hansen, L., Eilersten, R., Van Daele, M., De Batist, M., & Anselmetti, F. (2016). Moraine ridges in fjord-type, perialpine Lake Lucerne, central Switzerland. In J. A. Dowdeswell, M. Canals, M. Jakobsson, B. J. Todd, E. K. Dowdeswell, & K. A. Hogan (Eds.), *Atlas of Submarine Glacial Landforms: Modern, quaternary and ancient*. Geological Society Memoir, 46 (pp. 69–70). Geological Society of London.
- Lodolo, E., Lozano, J., Donda, F., Bran, D., Baradello, L., Romeo, R., Paterlini, M., Tassone, A., Grossi, M., Caffau, M., & Vilas, J. F. (in press). Holocene fluctuations of two southern Patagonia outlet glaciers revealed by high-resolution seismic surveys. *Quaternary Research*.
- Lozano, J. G., Tassone, A., Bran, D. M., Lodolo, E., Menichetti, M., Cerrredo, M. E., Esteban, F. D., Ormazabal, J. P., Isola, J., Baradello, L., & Vilas, J. F. (2018b). Glacial-related morphology and sedimentary setting of a high-latitude lacustrine basin: The Lago Chepelmut (Tierra del Fuego, Argentina). *Journal of South American Earth Sciences*, 86, 259–270. <https://doi.org/10.1016/j.jsames.2018.06.020>
- Lozano, J. G., Tassone, A., Lodolo, E., Menichetti, M., Cerrredo, M. E., Bran, D., Esteban, F., Ormazabal, J. P., Baradello, L., & Vilas, J. F. (2018a). Origin and evolution of Lago Yehuín (Tierra del Fuego, Argentina): Results from a geophysical survey. *Andean Geology*, 45(3), 318–343. <https://doi.org/10.5027/andgeoV45n3-3085>

- Mercer, J. H. (1968). Variations of some Patagonian glaciers since the late-Glacial. *American Journal of Science*, 266(2), 91–109. <https://doi.org/10.2475/ajs.266.2.91>
- Nullo, F. E., Blasco, G., Risso, C., Combina, A., & Otamendi, J. (2006). *Hoja Geológica 5172-I y 5175-II El Calafate, provincia de Santa Cruz*. Instituto de Geología y Recursos Minerales. Servicio Geológico Minero Argentino.
- Rabassa, J., Coronato, A., & Martinez, O. (2011). Late Cenozoic glaciations in Patagonia and Tierra del Fuego: An updated review. *Biological Journal of the Linnean Society*, 103(2), 316–335. <https://doi.org/10.1111/j.1095-8312.2011.01681.x>
- Renaut, R. W., & Gierlowski-Kordesch, E. H. (2010). Lakes. In N. James & R. Dalrymple (Eds.), *Facies Models* (4th edn., pp. 541–575). Geological Association of Canada.
- Skvarca, P., & Naruse, R. (1997). Dynamic behavior of Glaciar Perito Moreno, southern Patagonia. *Annals of Glaciology*, 24, 268–271. <https://doi.org/10.3189/S0260305500012283>
- Strelin, J. A., Denton, G. H., Vandergoes, M. J., Ninnemann, U. S., & Putnam, A. E. (2011). Radiocarbon chronology of the late-glacial Puerto Bandera moraines, southern Patagonian Icefield, Argentina. *Quaternary Science Reviews*, 30(19–20), 2551–2569. <https://doi.org/10.1016/j.quascirev.2011.05.004>
- Strelin, J. A., Kaplan, M. R., Vandergoes, M. J., Denton, G. H., & Schaefer, J. M. (2014). Holocene glacier history of the Lago Argentino basin, southern Patagonian Icefield. *Quaternary Science Reviews*, 101, 124–145. <https://doi.org/10.1016/j.quascirev.2014.06.026>
- Strelin, J. A., & Malagnino, E. C. (1996). Glaciaciones pleistocenas del Lago Argentino y alto valle del Río Santa Cruz. In *Actas del XIII Congreso Geológico Argentino* (Vol. 4, pp. 311–325), Buenos Aires: Asociación Geológica Argentina.
- Waldmann, N., Ariztegui, D., Anselmetti, F. S., Coronato, A., & Austin, J. A. Jr. (2010). Geophysical evidence of multiple glacier advances in Lago Fagnano (54°S), southernmost Patagonia. *Quaternary Science Reviews*, 29(9–10), 1188–1200. <https://doi.org/10.1016/j.quascirev.2010.01.016>
- Wessel, P., & Smith, W. H. (1991). Free software helps map and display data. *Eos, Transactions American Geophysical Union*, 72(41), 441–446.
- Yilmaz, Ö. (2001). *Seismic data analysis: Processing, inversion, and interpretation of seismic data*. Society of exploration geophysicists.